Different target specificities of haptoglobin and hemopexin define a sequential protection system against vascular hemoglobin toxicity

Deuel, Jeremy W ; Vallelian, Florence ; Schaer, Christian A ; Puglia, Michele ; Buehler, Paul W ; Schaer, Dominik J

Abstract: Free hemoglobin (Hb) triggered vascular damage occurs in many hemolytic diseases, such as sickle cell disease, with an unmet need for specific therapeutic interventions. Based on clinical observations the Hb and heme scavenger proteins haptoglobin (Hp) and hemopexin (Hx) have been characterized as a sequential defense system with Hp as the primary protector and Hx as a backup when all Hp is depleted during more severe intravascular hemolysis. In this study we present a mechanistic rationale for this paradigm based on a combined biochemical and cell biological approach directed at understanding the unique roles of Hp and Hx in Hb detoxification. Using a novel in vitro model of Hb triggered endothelial damage, which recapitulates the well-characterized pathophysiologic sequence of oxyHb(Fe2+) transformation to ferric Hb(Fe3+), free heme transfer from ferric Hb(Fe3+) to lipoprotein and subsequent oxidative reactions in the lipophilic phase. The accumulation of toxic lipid peroxidation products liberated during oxidation reactions ultimately lead to endothelial damage characterized by a specific gene expression pattern with reduced cellular ATP and monolayer disintegration. Quantitative analysis of key chemical and biological parameters allowed us to precisely define the mechanisms and concentrations required for Hp and Hx to prevent this toxicity. In the case of Hp we defined an exponential relationship between Hp availability relative to oxyHb(Fe2+) and related protective activity. This exponential relationship demonstrates that large Hp quantities are required to prevent Hb toxicity. In contrast, the linear relationship between Hx concentration and protection defines a highly efficient backup scavenger system during conditions of large excess of free oxyHb(Fe2+) that occurs when all Hp is consumed. The diverse protective function of Hp and Hx in this model can be explained by the different target specificities the two proteins.

DOI: https://doi.org/10.1016/j.freeradbiomed.2015.09.016

Deuel, Jeremy W; Vallelian, Florence; Schaer, Christian A; Puglia, Michele; Buehler, Paul W; Schaer, Dominik J (2015). Different target specificities of haptoglobin and hemopexin define a sequential protection system against vascular hemoglobin toxicity. Free Radical Biology Medicine, 89:931-943.
DOI: https://doi.org/10.1016/j.freeradbiomed.2015.09.016

Free Radical Biology and Medicine 89 (2015) 931–943

Contents lists available at ScienceDirect

Free Radical Biology and Medicine

journal homepage: www.elsevier.com/locate/freeradbiomed

Original Contribution

Different target specificities of haptoglobin and hemopexin define a sequential protection system against vascular hemoglobin toxicity

Jeremy W. Deuel [a], Florence Vallelian [a], Christian A. Schaer [a], Michele Puglia [a,b], Paul W. Buehler [c], Dominik J. Schaer [a,*]

[a] Division of Internal Medicine, University Hospital of Zurich, Switzerland
[b] Functional Genomics Center, University of Zurich, Switzerland
[c] Center of Biologics Evaluation and Research (CBER), FDA, Silver Spring, Maryland, USA

ARTICLE INFO

Article history:
Received 22 May 2015
Received in revised form
31 July 2015
Accepted 20 September 2015
Available online 22 October 2015

Keywords:
Hemolysis
Hemoglobin
Haptoglobin
Hemopexin
Lipoprotein
Lipid oxidation
Endothelial cell

ABSTRACT

Free hemoglobin (Hb) triggered vascular damage occurs in many hemolytic diseases, such as sickle cell disease, with an unmet need for specific therapeutic interventions. Based on clinical observations the Hb and heme scavenger proteins haptoglobin (Hp) and hemopexin (Hx) have been characterized as a sequential defense system with Hp as the primary protector and Hx as a backup when all Hp is depleted during more severe intravascular hemolysis. In this study we present a mechanistic rationale for this paradigm based on a combined biochemical and cell biological approach directed at understanding the unique roles of Hp and Hx in Hb detoxification. Using a novel in vitro model of Hb triggered endothelial damage, which recapitulates the well-characterized pathophysiologic sequence of oxyHb(Fe^{2+}) transformation to ferric Hb(Fe^{3+}), free heme transfer from ferric Hb(Fe^{3+}) to lipoprotein and subsequent oxidative reactions in the lipophilic phase. The accumulation of toxic lipid peroxidation products liberated during oxidation reactions ultimately lead to endothelial damage characterized by a specific gene expression pattern with reduced cellular ATP and monolayer disintegration. Quantitative analysis of key chemical and biological parameters allowed us to precisely define the mechanisms and concentrations required for Hp and Hx to prevent this toxicity. In the case of Hp we defined an exponential relationship between Hp availability relative to oxyHb(Fe^{2+}) and related protective activity. This exponential relationship demonstrates that large Hp quantities are required to prevent Hb toxicity. In contrast, the linear relationship between Hx concentration and protection defines a highly efficient backup scavenger system during conditions of large excess of free oxyHb(Fe^{2+}) that occurs when all Hp is consumed. The diverse protective function of Hp and Hx in this model can be explained by the different target specificities of the two proteins.

1. Introduction

Hemoglobin (Hb) release from red blood cells (RBC) is a common pathophysiology of many disorders. Systemic hemolysis occurs during certain genetic and acquired anemia, such as in sickle cell disease and malaria. Localized Hb release occurs at confined sites of tissue injury, inflammation, or within atherosclerotic plaques. Depending on the scale, rate, and site of hemolysis, the primary adverse effects triggered by free Hb are vascular dysfunction, oxidative tissue damage, and altered inflammatory response [1–6].

The Hb and heme scavenger proteins haptoglobin (Hp) and hemopexin (Hx) exhibit high binding rate constants for Hb [7] and heme [8], respectively. Both in vitro and in vivo studies have demonstrated the ability of these proteins to attenuate Hb and heme-induced toxicity [9–11]. Under physiologic conditions Hp and Hx exist at comparable plasma concentrations and both are depleted from plasma after binding Hb or heme, respectively. However, in patients with hemolysis Hp depletes early in the course of the disease while levels of Hx remain within the physiologic range for prolonged periods of sustained hemolytic disease [12]. Based on these observations, the two proteins have been characterized as constituents of a sequential Hb/heme protection system with Hp as the primary defense and Hx as the backup, which provides protection against more severe Hb exposure once Hp becomes depleted [12,13]. The biochemical basis of this paradigm of sequential protection by Hp and Hx has yet to be explored systematically.

The vasculature is one of the principal targets of Hb toxicity [14]. Many studies have explored basic mechanisms of Hb or heme

* Correspondence to: University Hospital of Zurich Division of Internal Medicine Rämistrasse 100 8091 ZurichSwitzerland. Tel.: +41 44 2552382.
E-mail address: dominik.schaer@usz.ch (D.J. Schaer).

http://dx.doi.org/10.1016/j.freeradbiomed.2015.09.016

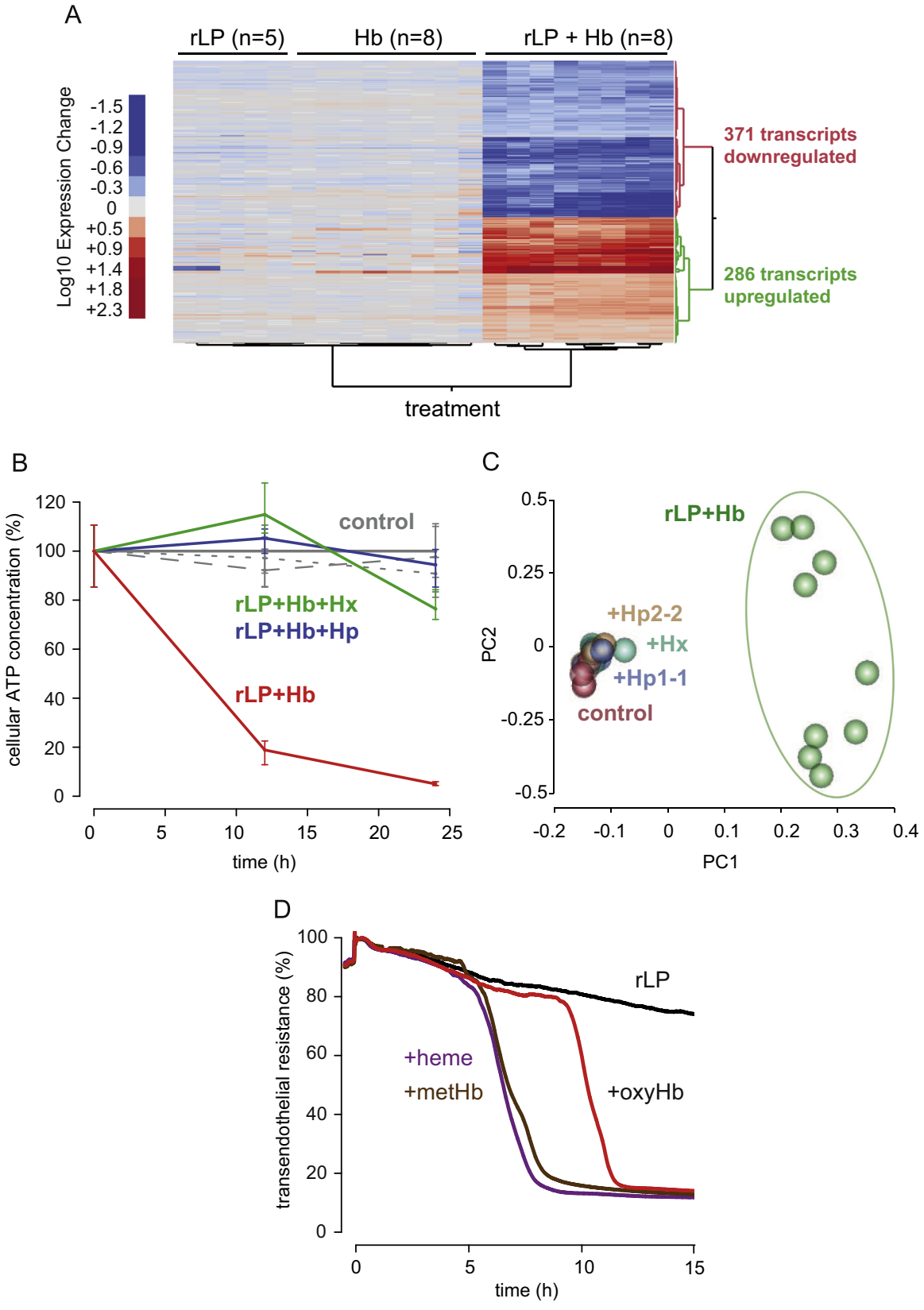

Fig. 1. Effects of combined treatment of rLP and Hb on human umbilical vein endothelial cells. A. Hierarchical two-way clustering analysis of whole genome expression arrays. HUVEC where treated for 9 h with rLP (0.5 mg/ml), Hb (10 μM), or both. Only genes found to exhibit statistically significant differential regulation by ANOVA are shown. The clustering indicates clear separation of the treatment conditions with most pronounced gene expression changes for combined rLP+Hb treatment. Details of gene expression data can be found in the data supplement. B. Time course of cellular ATP depletion. The rLP (0.5 mg/ml)+Hb (10 μM) triggered damage response in HUVEC cells is prevented by Hp and Hx added at excess concentration over Hb (each at 15 μM heme-equivalent binding capacity). C. Principal component analysis of gene expression profiles of untreated HUVEC or HUVEC treated with rLP+Hb in the absence of any scavenger or with Hx or Hp of dimeric or multi-meric phenotype (Hp 1–1 and Hp 2–2). The data confirm that the Hb+rLP triggered gene expression changes are prevented by Hx and Hp. The axes indicate principal components (PC1 and PC2). D. Electric cell-substrate impedance sensing (ECIS) of HUVEC treated with rLP alone or in combination with heme, metHb (Fe3+), or oxyHb (Fe2+). rLP in combination with oxyHb leads to disruption of endothelial monolayer integrity after about 10 h. If oxyHb is replaced by ferric Hb or free heme, the time to disruption is shortened to about 6 h. Single treatment with heme, oxyHb or ferric Hb does not change monolayer integrity (not shown).

triggered endothelial damage and have suggested that oxidative reactions of Hb generate multiple toxic species such as free heme that is released from ferric Hb, iron, free radicals, and globin aggregation products [15–25]. Toxic reaction products such as oxidized lipoproteins are formed in secondary reactions [19,26]. Therefore, the well-characterized sequence of Hb triggered endothelial toxicity is a relevant pathophysiologic situation to quantitatively evaluate differential protective scavenger protein requirements of Hp and Hx during Hb exposure.

Here we present a novel in vitro model of Hb-mediated endothelial toxicity, which recapitulates the established sequence of heme iron oxidation from ferrous Hb (Fe^{2+}) to ferric Hb (Fe^{3+}), heme release from ferric Hb, and heme-driven oxidation of unsaturated fatty acids as the critical mechanism driving Hb-induced endothelial damage. Unlike previous studies that focus on individual contributions of Hp or Hx irrespective of concentration dependence, within this global model we identified measures of Hb/lipid oxidation and endothelial damage, which allowed us to quantitatively define scavenger protein requirements of Hp and Hx in relation to the amount of oxyHb (Fe^{2+}) present in the system. Our data show that at least iso-stoichiometric quantities of the primary scavenger Hp in relation to oxyHb (Fe^{2+}) are required to provide full protection. In contrast, sub-stoichiometric quantities of the backup scavenger Hx are sufficient to significantly attenuate Hb triggered lipid oxidation and endothelial damage in the absence of Hp.

2. Materials and METHODS

2.1. Chemicals and concentrations

Purified Hb was further processed by DEAE ion exchange chromatography to remove catalase and other antioxidant enzymes. After purification Hb was in the oxyHb(Fe^{2+}) sate with no detectable ferric Hb(Fe^{3+}). Throughout this article, molar quantities of Hb relate to total heme, which is equivalent to the single chain subunits of Hb (alpha or beta chain). For the scavenger proteins (Hx and Hp), we considered one mole as the binding capacity equivalent for one mole of heme, considering that one Hp αβ-subunit ($\approx$42 kD) can bind two heme molecules (corresponding to one αβ-dimer), while a Hx molecule ($\approx$57 kD) can bind one heme molecule. Hb concentration was measured by spectrophotometry using a molar extinction coefficient of 524.3 $M^{-1}\,cm^{-1}$ at an absorbance wavelength of 414 nm (for oxyHb).

Ferric Hb (Fe^{3+}) was generated by incubating oxyHb (Fe^{2+}) with a five times molar excess of $K_3[Fe(CN)_6]$ in PBS, pH 7.45 at room temperature for 10minutes followed by removal of $K_3[Fe(CN)_6]$ by size exclusion separation on a PD-10 column (GE Healthcare). Ferric Hb concentration and complete oxidation to ferric iron (Fe^{3+}) within Hb where then determined by spectrophotometry.

Heme was dissolved in 5 ml DMSO at a concentration of 10 mM and then 5 ml of 1 M NaOH was added. The solution was mixed vigorously and then dissolved to a final stock concentration of 1 mM with PBS. This stock solution was immediately frozen and stored at -20°C until use. Additional freeze-thaw cycles were avoided.

Human plasma derived Hp (predominantly phenotype 2–2) and Hx were provided by CSL Behring (Bern, Switzerland). For the experiment shown in Fig. 1C we additionally used an Hp product from BPL Bio Products Laboratories, which is predominantly phenotype 1–1. The purity of the proteins was analyzed by gel electrophoresis (Supplemental Figure 1) and by LC-MSMS. The irreversible Hb binding function of Hp was confirmed by surface plasmon resonance (SPR). Heme binding of Hx was confirmed by spectrophotometry, which shows a specific spectrum for the Hx-heme complex [7]. Concentrations of binding-proteins were measured by spectrophotometry at 280 nm using a molar extinction coefficient of 25.8 $mM^{-1}\,cm^{-1}$ for Hp and 116 $mM^{-1}\,cm^{-1}$ for Hx.

Reconstituted lipoprotein (rLP; CSL-111) was obtained from CSL Behring (Switzerland) [27]. rLP was reconstituted in PBS to a final stock concentration of 40 g/l and immediately aliquoted and stored at −80 °C until use. For rLP, all given concentrations are relative to the $apoA_1$-lipoprotein concentration. The lipoprotein is composed of human plasma derived apoA-I lipoprotein and lecithin with phosphatidylcholine as the principal lipid component.

2.2. Cell culture experiments

Human umbilical vein endothelial cells (HUVEC) were obtained from Lonza (Switzerland) and cultured in EGM medium (Lonza) under standard conditions. All experiments were conducted in complete EGM without ascorbic acid with cells forming a confluent monolayer.

2.3. Gene expression microarray experiments and data analysis

RNA preparation and quality control was performed as reported earlier [28]. Fluorescently labeled cRNA was generated from 500 ng total RNA using the Quick Amp Labeling Kit (Agilent Technologies, Basel, Switzerland) according to the manufacturer's protocol, and differential gene expression profiling was performed by competitive dual-color hybridization on Whole Human Genome Oligo Microarrays (G4845A, 4 × 44K, 60-mer, Agilent Technologies). Array slides were XDR scanned and analyzed with Feature Extraction Software Version 10.7.3.1 (Agilent Technologies). Statistical analysis and visualization were performed with JMP Genomics 5.0 (SAS). Specified clusters of regulated genes were analyzed for enrichment of functional networks by using Metacore analysis software (Thomson Reuters).

2.4. Electrical cell impedance sensing (ECIS) and ATP measurement

Confluent HUVEC cells grown in one 10- cm tissue culture plate were trypsinized and plated into two 8W10E+ ECIS plates filled with 400 μl medium per well. Cells were allowed to settle for 24 h, and then the medium was changed to 300 μl per well. After 2–5 h, when the ECIS-signal stabilized, 100 μl of pre-warmed 4x treatment was added directly to the wells while running the ECIS acquisition at 4 kHz. The signal was then normalized to 30 min before treatment. The amount of time required to lose endothelial monolayer integrity was calculated by finding the minimum in the first derivate of the measured resistance over time.

Cellular ATP was measured with a chemiluminescent assay (CellTiter-Glo® Assay, Promega AG, Dubendorf, Switzerland). Experiments were performed in 96-well plates, and luminescence was measured with an Infinite M200-Pro plate reader (Tecan Group Ltd., Männedorf, Switzerland).

2.5. Spectrophotometry

Experiments were conducted in 1 ml semi-micro cuvettes at 37 °C using a Cary 60 spectrophotometer (Agilent, Switzerland). Absorbance was measured over time at every 2 nm between 350 to 650 nm with a 0.025 s integration time per wavelength. Spectra were deconvoluted against standard extinction curves of the pure substances using a non-negative least squares algorithm. The time to oxygen depletion was calculated as the minimum of the first derivative of the oxyHb concentration over time.

2.6. Simultaneous oxygen concentration measurement during spectrophotometry

rLP was incubated at 0.5 g/l in PBS, pH 7.45 with 10 μM oxyHb at 37 °C. Oxygen content was measured with an O_2 microsensor placed directly in the spectrophotometry cuvette and recorded with SensorTrace Pro Software (both from Unisense, Aarhus, Denmark). Oxygen sO_2 was calculated for the measured oxygen concentration using the Kelman [29] formula adjusted for a pCO_2 of 0.

2.7. Measurement of thiobarbituric acid reactive substances (TBARS)

A 100 μl aliquot of the sample was diluted in 500 μl of 750 mM trichloracetic acid in 1 M HCl. After vortexing, 400 μl of a 25 mM solution of 2-thiobarbituric acid in 1 M NaOH was added and then the sample was incubated for 60 min at 80 °C. After pelleting debris, TBARS were quantified in the supernatant. For absolute quantification, the absorption at 532 nm (thereof subtracted the absorption at 600 nm) was used to calculate the concentration with the extinction coefficient of 0.156 $\mu M^{-1}\,cm^{-1}$ using a 1- cm pathlength cuvette. For a more sensitive but relative quantification, we measured the fluorescence emission at 590 nm using 540 nm as the excitation wavelength.

2.8. Detection of 4-hydroxynonenal protein adducts be Western blot

rLP (0.5 g/l) with or without Hb (50 μM), Hx (10 μM) or Hp (10 μM or 50 μM) was incubated for 120 min at 37 °C in PBS pH 7.4. The reaction was stopped by addition of the same volume of Lämmli-Buffer containing 5% beta-mercaptoethanol, samples were boiled for 5 min at 95 °C, spun down and 10 μl per lane run on a Criterion Any-KD Stain-Free gel (Bio-Rad). The gel was activated during 1 min under UV-Light and then blotted onto a PVDF-Membrane. After blocking with PBS containing 10 g/l BSA, 10% goat-serum and 0.1% Tween-20 over night, the mouse monoclonal anti-hydroxynonenal-antibody (MAB3249, RD-Systems) was incubated for 1 hour at 1 mg/l concentration followed by an Alexa-Fluor-660 anti-mouse IgG antibody (Life Technologies) for another hour. The blot was visualized on a Chemidoc MP imager (Bio-Rad).

2.9. Lipid Mass Spectrometry (LMS)

0.5 g/l rLP was reacted with Hb for 2 h at 37 °C (oxidized rLP). As a control, rLP was incubated under the same conditions in the absence of heme (non-oxidized rLP). To extract the lipids, we used a modified method based on Matyash [30]. Briefly, 200 μl of each sample was added to 1.5 ml of methanol containing 50 mg/l butylated hydroxytoluene (BHT) in a 15 ml borosilicate glass test tube. After mixing, 5 ml of methyl tert-butyl ether was added and extracted for 60 min at room temperature by vigorous shaking followed by the addition of 1.25 ml of water and incubation for another 10 min. After centrifugation at $1{,}000 \times g$ for 10 min, the upper phase was transferred to a new glass tube and dried under a steady flow of nitrogen at 37 °C. The dry lipid pellet was re-suspended using 0.5 ml of methanol and agitated for 20 min. Samples were then stored at 4 °C in 2 ml amber glass vials (SUPELCO, Bellefonte, PA, USA) until the next step. Immediately before mass spectrometric analysis, lipids were diluted 1:5 in a solution containing 10 mM ammonium acetate in 80% methanol and analyzed by reverse phase chromatography on a Q-Exactive mass spectrometer (Thermo Fisher Scientific, Bremen, Germany) coupled to a nanoACQUITY UPLC® system (Waters, Milford, MA, USA). Lipids were automatically selected by an auto-sampler and successively separated on a 5 cm-long fused silica emitter column (200 μm i.d.; BGB Analytik, Boeckten, Switzlerand) and in-house packed with HSS T3, 100 Å, 1.8 μm, C18 resin (Waters). The chromatographic separation was performed using a 2-propanol:ACN/water solvent system containing 5 mM ammonium acetate at a flow rate of 2 ul/min. A gradient from 2% to 98% 2-propanol:ACN in 10minutes was used. The total run time was 22 min, which also included sample injection and column equilibration. Mass spectra were acquired in a data-dependent manner with an automatic switch between MS and MS/MS using a top 5 method. MS spectra were acquired using the Orbitrap analyzer with a mass range of 80–1200 m/z and 70,000 resolution at m/z 200. HCD lipid fragments were obtained using a stepped normalized collision energy of 20–30 with an AGC target value of 5×104 at 17,500 resolution. The isolation window was set to 0.4 Da. Dynamic exclusion ($\pm$ 10 ppm tolerance) was used with one repeat count and a 6 s exclusion duration. Measurements were performed using an internal lock mass calibration on m/z 371.10124 and 445.12003. Chromatograms of selected MS1 ions were extracted using Xcalibur software (Thermo Fisher Scientific, USA). Comparative m/z-RT plots were generated by aligning two images produced using the Pep3D software (TPP, Seattle Proteome Center) by FIJI (www.fiji.sc).

2.10. Statistical analysis

Unless otherwise indicated, all statistical analyses, model generation, and fitting were performed using the R statistical software (www.r-project.org).

3. RESULTS

3.1. An in vitro model of Hb lipoprotein-triggered endothelial toxicity

Hb is a known oxidizer of lipoprotein (LP) [6]. Oxidized LP (ox-LP) then induces toxic effects in endothelial cells [6]. Because of the variability of lipid and intrinsic anti-oxidant composition in plasma-derived LP, previous models of Hb triggered lipid oxidation have used free heme (a stronger oxidant), bolus addition, or in situ enzymatic generation of H_2O_2 to produce a sufficiently strong oxidative drive to overcome the unpredictability of oxyHb (Fe^{2+}) oxidative reactions [16,18,19,21]. These systems have clear limitations for the modeling of scavenger protein effects during hemolytic conditions, which are always characterized by an excess of ferrous Hb with relatively mild oxidative stress [9]. The in vitro model presented herein, replaces natural LP with a reconstituted lipoprotein (rLP) composed of apoA-I lipoprotein, which serves as a stabilizer of the LP particle, in conjunction with a defined lipid component composed of saturated and unsaturated fatty acids in the form of phosphatidylcholine (PC), absent anti-oxidants. We hypothesized that this rLP lipid component would react spontaneously and more predictably with ferrous Hb to produce oxidized LP (ox-LP) and Hb oxidation products and then eventually yield toxic end-products.

Fig. 1**A** shows results from a whole genome microarray analysis that was performed on human umbilical vein endothelial cells (HUVEC) treated with 0.5 g/l rLP + 10 μM oxyHb(Fe^{2+}) or either compound alone. Gene array data are accessible at NCBI's Gene Expression Omnibus under http://www.ncbi.nlm.nih.gov/geo/query/acc.cgi?acc=GSE66283 and in the data supplement. Hierarchical clustering analysis demonstrates that dramatic changes in gene expression were induced by combined treatment with rLP and Hb in complete culture medium compared to the individual compounds. In particular, 286 transcripts were up-regulated by rLP + oxyHb (Fe^{2+}), while 371 were down-regulated. A Metacore® gene enrichment analysis for biological processes suggested activation of the response to unfolded proteins and apoptosis triggered by the MAPK and JAK/STAT pathways. This gene expression

response was associated with a decrease in cellular ATP (Fig. 1**B**). Both, the gene expression response and the drop in cellular ATP were completely blocked by Hp and Hx when added in excess over heme concentration (Fig. 1**B/C**). rLP+Hb disrupted the endothelial barrier integrity, measured by ECIS, within 12hours. In contrast, exposure to either rLP or Hb alone did not change endothelial resistance (Fig. 1**D**). Compared to the effect of oxyHb (Fe^{2+}) the cytotoxic effect of rLP+Hb was accelerated to approximately twice the rate following replacement of oxyHb (Fe^{2+}) with ferric Hb (Fe^{3+}). Identical acceleration was observed when ferric Hb (Fe^{3+}) was replaced by an iso-stoichiometric amount of free heme, indicating that the globin component of Hb is not directly involved in the cytotoxic response in this model. No significant effect on endothelial barrier integrity was observed when the cells were incubated with ferric Hb(Fe^{3+}) or heme alone. These data are supported by immunofluorescence staining for β-catenin, which demonstrate disintegration of endothelial adherence junctions following treatment with either rLP+oxyHb (Fe^{2+}), rLP+ferric Hb (Fe^{3+}) or rLP+heme. These effects were blocked by the addition of excess concentrations of Hp and Hx (Fig. 2).

3.2. Biochemical characterization of the Hb-lipoprotein reaction

Using spectrophotometry combined with spectral deconvolution, we evaluated the dynamic changes in Hb oxygenation and heme-iron redox states that occurred when 10 μM oxyHb (Fe^{2+}) was reacted with 0.5 g/l rLP (Fig. 3**A**). The aim of these initial biochemical experiments was to define key parameters for quantitative characterization of the cytoprotective effects of Hp and Hx in later experiments. During the reaction, conversion from oxyHb to deoxyHb occurred after 20 min. Around this time point, the concentration of ferric Hb (Fe^{3+}) and ferryl Hb (Fe^{4+}) increased. These data are suggestive of an oxygen-consuming reaction characteristic of singlet oxygen ($^1O_2$)-mediated lipid oxidation. The time-point at which Hb became desaturated was used in subsequent experiments as a marker of the reaction velocity and its modulation. To verify the spectral deconvolution data, we measured the oxygen consumption rate during the reaction with a Clark-type electrode and calculated Hb oxygen saturation (sO_2) (Fig. 3**B**). sO_2 calculated from the measured oxygen concentration and by spectrophotometry showed very similar results, demonstrating the accuracy of our spectrophotometric method for monitoring oxygen consumption by the rLP-Hb reaction.

Accumulation of rLP-derived lipid oxidation products was confirmed by LC-MS/MS. Fig. 4**A** shows a representative 2D plot of retention time versus m/z with an in silico overlay of a control rLP sample and an rLP sample that was treated with oxyHb for 8 h at 37 °C. In this overlay, white indicates the products present in both samples, while magenta represents products of the rLP-Hb reaction. The appearance of magenta species with progressively higher m/z and lower retention time (=higher polarity) is compatible with the generation of multiple lipid oxidation products that are characterized by serial oxygen adduction.

To confirm this hypothesis, we identified within the dataset specific phosphatidylcholines (PC), which constitute the major component of rLP, and searched for putative oxidized forms of these lipids. The structural formula of an exemplary polyunsaturated PC (1-octadecatrienoyl-2-octadecenoyl-sn-glycero-3-phosphocholine) is depicted in Fig. 4**B**. The single-ion trace of the non-oxidized PC present at the onset of the reaction was extracted

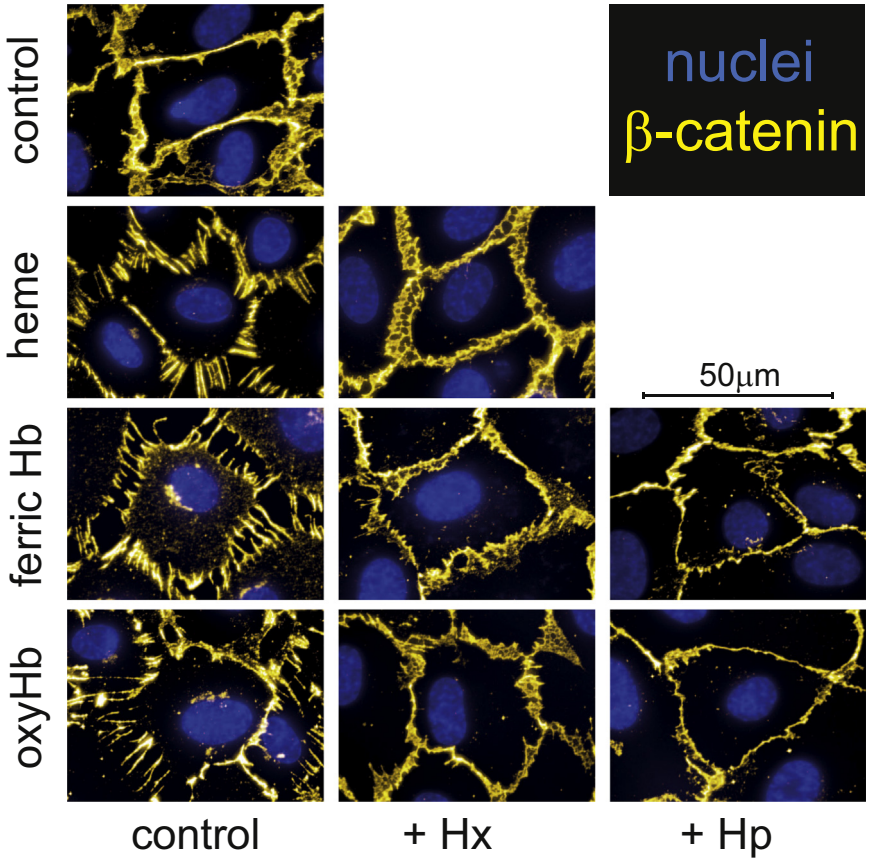

Fig. 2. Hp and Hx prevent endothelial adherence junction disruption induced by rLP+Hb treatment. Immunofluorescence images of HUVEC stained for β-catenin (yellow, Alexa-555 fluorescence). HUVEC were treated for 6 h with rLP alone (control) or rLP+oxyHb, +metHb, or +heme in the absence or presence of Hx or Hp. Note the spiculated pattern of beta-catenin staining in all treatments including unprotected heme or Hb.

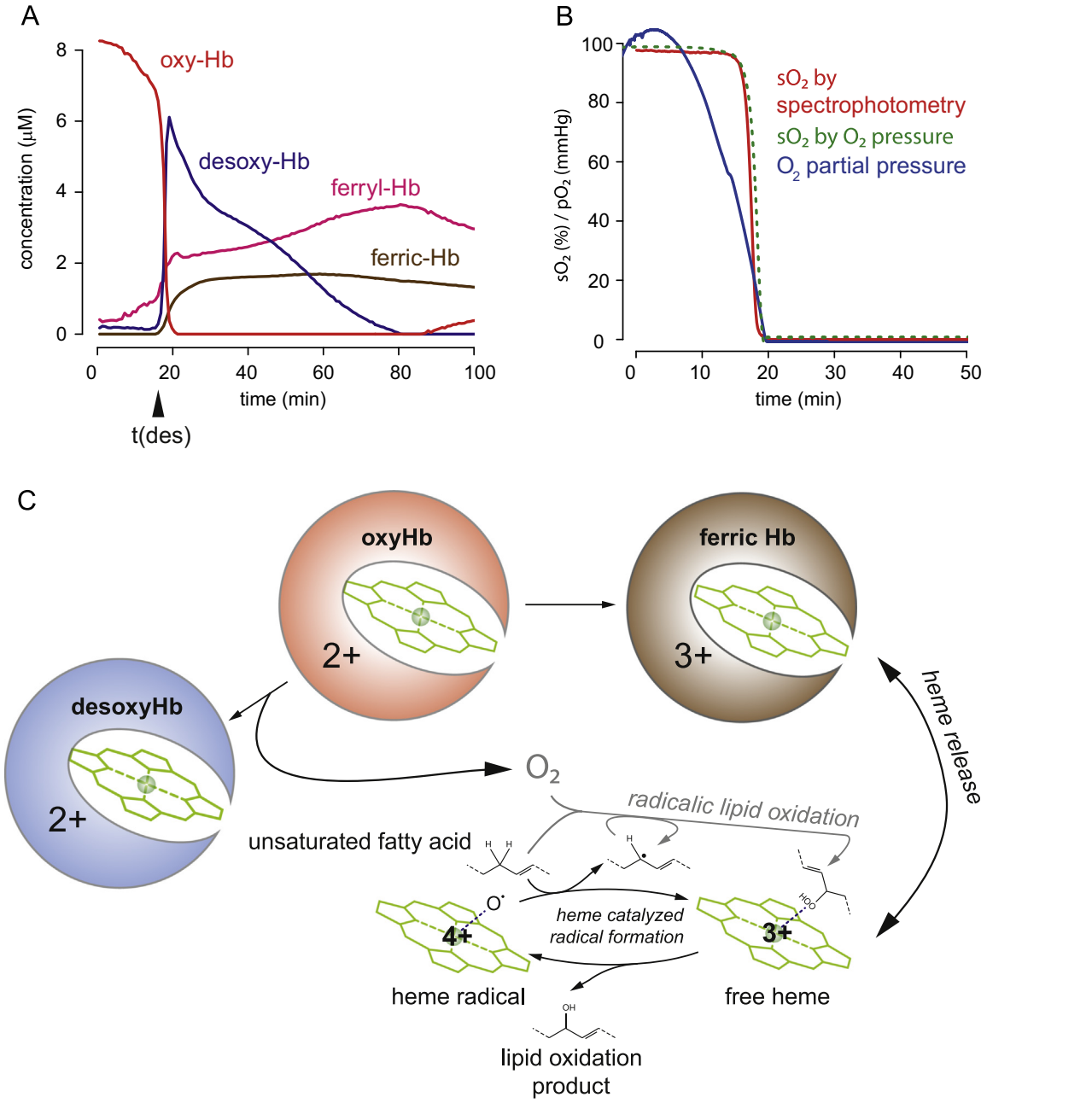

Fig. 3. Hb oxygenation and oxidation state kinetics during the reaction with rLP. A. Time course of different Hb oxygenation and oxidation states during the reaction of oxyHb with rLP (rLP 0.5 g/L, oxyHb (Fe2+) 10 μM, PBS pH 7.4, 37°C) as observed by spectrophotometry and spectral deconvolution. The Hb desaturation time (tdes) is indicated by the triangle. B. Verification of oxygen depletion by direct measurement of oxygen pressure. Using the same sample as in (A) we determined the percentage of sO2 by multi-compound spectrophotometric deconvolution (red) and direct measurement of oxygen pressure (green). C. Proposed mechanism for Hb triggered lipid peroxidation. As a first event a small fraction oxyHb (Fe2+) is oxidized to ferric Hb (Fe3+). Heme is released from ferric Hb, which is therefore considered a free heme equivalent. Heme will accumulate in the lipid compartment and catalyze lipid peroxidation in an oxygen-dependent reaction. While oxygen is consumed by the reaction, the remaining oxyHb is desaturated to desoxyHb. Hb desaturation can therefore be measured as an indicator of the Hb triggered oxygen consuming lipid peroxidation.

and plotted versus retention time (Fig. 4**C**, black trace). A series of oxygen adduction products of this PC, which are defined by characteristic mass (15.9949 u=+1 oxygen) and retention time shifts (increased polarity), were identified (colored traces) along with the non-oxidized precursor PC in the rLP+Hb reaction. These oxidized forms were not present in the rLP prior to Hb triggered oxidation.

From the previous experiments, it was unclear whether endothelial changes following rLP+Hb exposure in our model were caused by oxidized rLP species, free heme, or mechanisms that involved short-lived reaction intermediates such as free radicals or ferryl iron (Fe^{4+}). Only toxicity due to globin oxidation products could be excluded because Hb could be replaced with heme (as shown in Fig. 1**D**). Therefore, to identify the cytotoxic species, we incubated endothelial cells with rLP that had been pre-reacted with heme and then depleted of free heme immediately prior to cell exposure by addition of excess Hx (Fig. 4**D**). The immediate cytotoxicity of this reaction product, which occurred without the typical lag-time, suggests that the accumulated lipid oxidation products are the ultimate mediator of toxicity. As a control, endothelial cells were treated with rLP that was incubated with heme+Hx throughout the experiment including the pre-incubation period. Due to the irreversible binding of Hx to heme, lipid oxidation did not occur and cytotoxicity was not observed.

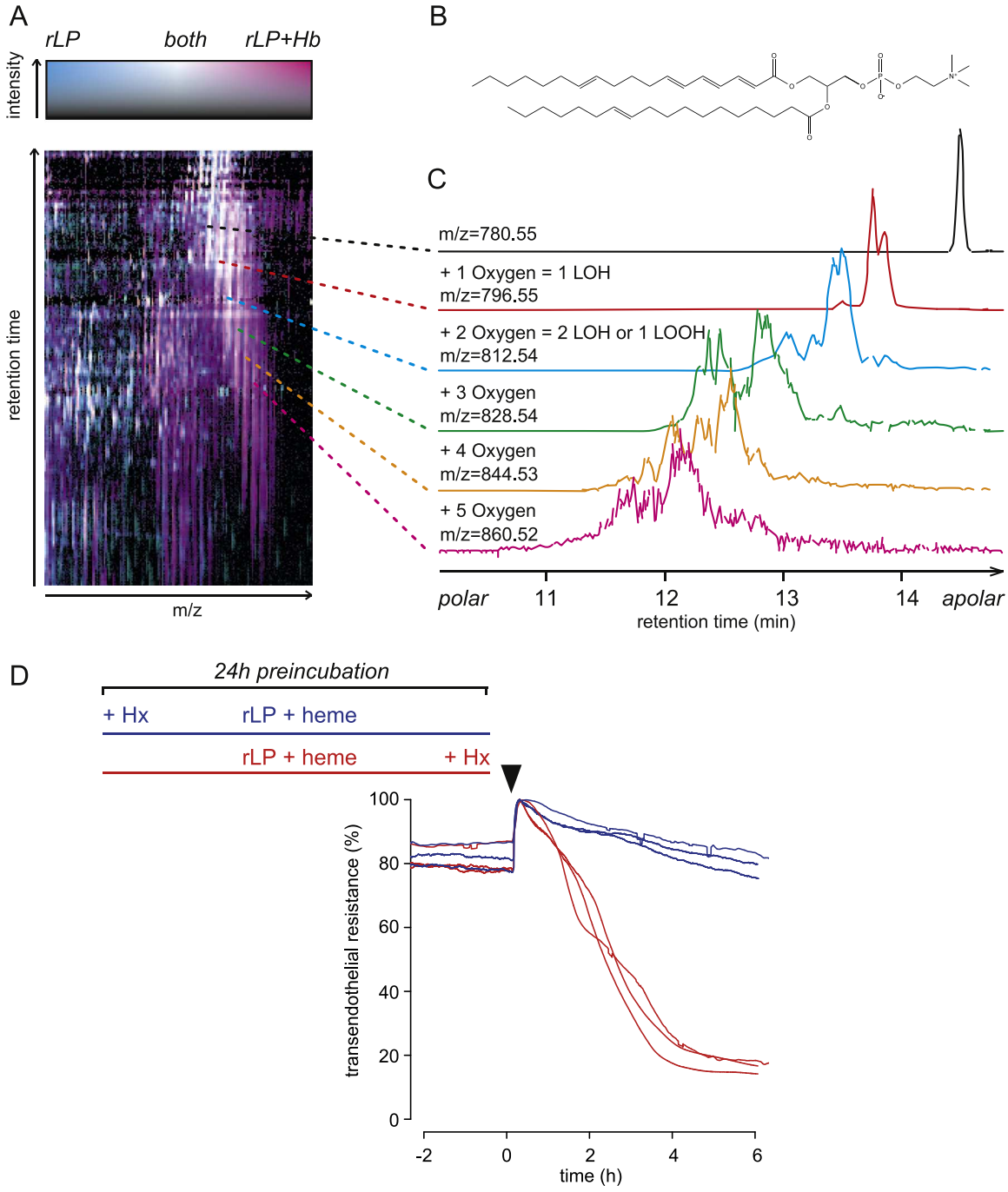

Fig. 4. The rLP+Hb reaction generates toxic lipid oxidation products. A. Overlay of two m/z x retention time plots of all compounds that were detected by LC-MSMS in native rLP (cyan) and heme-treated rLP (magenta). Compounds appearing cyan were more abundant in the native rLP sample whereas compounds appearing magenta were more abundant in the Hb-treated sample. Compounds appearing white were found in both samples. The right shifted population (increased m/z) of magenta colored compounds in the rLP+Hb samples is compatible with oxidation (oxygen adduction, increased mass). The y-axis is the retention time, where more polar (i.e. oxygen adducted/ oxidized compounds in the rLP+Hb sample) compounds are further down (lower retention time) and more apolar, lipophilic substances are further up (higher retention time). The dashed lines to panel C indicate the area where the main intensity peak of the single-ion chromatograms shown in Fig. 4C were located. Overall the right/down shifted cloud of compounds in the rLP+Hb samples is compatible with extensive oxidative lipid modifications. B. Structure of the exemplary phosphatidylcholine 1-octadeca-2,4,6-trienoyl-2-octadeca-11-enoyl-sn-glycero-3-phosphocholine PC(18:3[2,4,6]/18:1[11]) in its unoxidized form. C. Single-ion chromatograms of native and oxygen adducted PC (18:3[2,4,6]/18:1[11]) extracted from native and Hb reacted rLP, respectively. The native lipid is shown in black ([M-H]- ion), while all other ions (colored traces) are depicted as putative oxidized species identified by an increase in m/z by one oxygen mass and decrease in retention time to increased polarity. The most oxidized species were exclusively detected in Hb treated rLP. D. ECIS experiment measuring endothelial monolayer integrity of confluent HUVEC treated with heme-catalyzed lipid peroxidation products. Cells were treated with rLP that was pre-incubated with heme for 24 h and then captured with Hx to remove remaining free heme (red). As a control, cells were treated with rLP incubated with heme that was already captured with Hx during the whole pre-incubation period (blue).

3.3. *Free heme transfer from ferric Hb (Fe^{3+}) into rLP*

Next, we performed studies to identify the reaction intermediates that promote rLP oxidation in our model following the addition Hb. Fig. 5**A** illustrates that addition of free heme to the oxyHb (Fe^{2+})+rLP reaction accelerates oxygen consumption, which is observed by a shorter time to $t_{desaturation}$. Addition of equimolar amounts of ferric Hb (Fe^{3+}) yielded identical results as addition of free heme. Ferric Hb

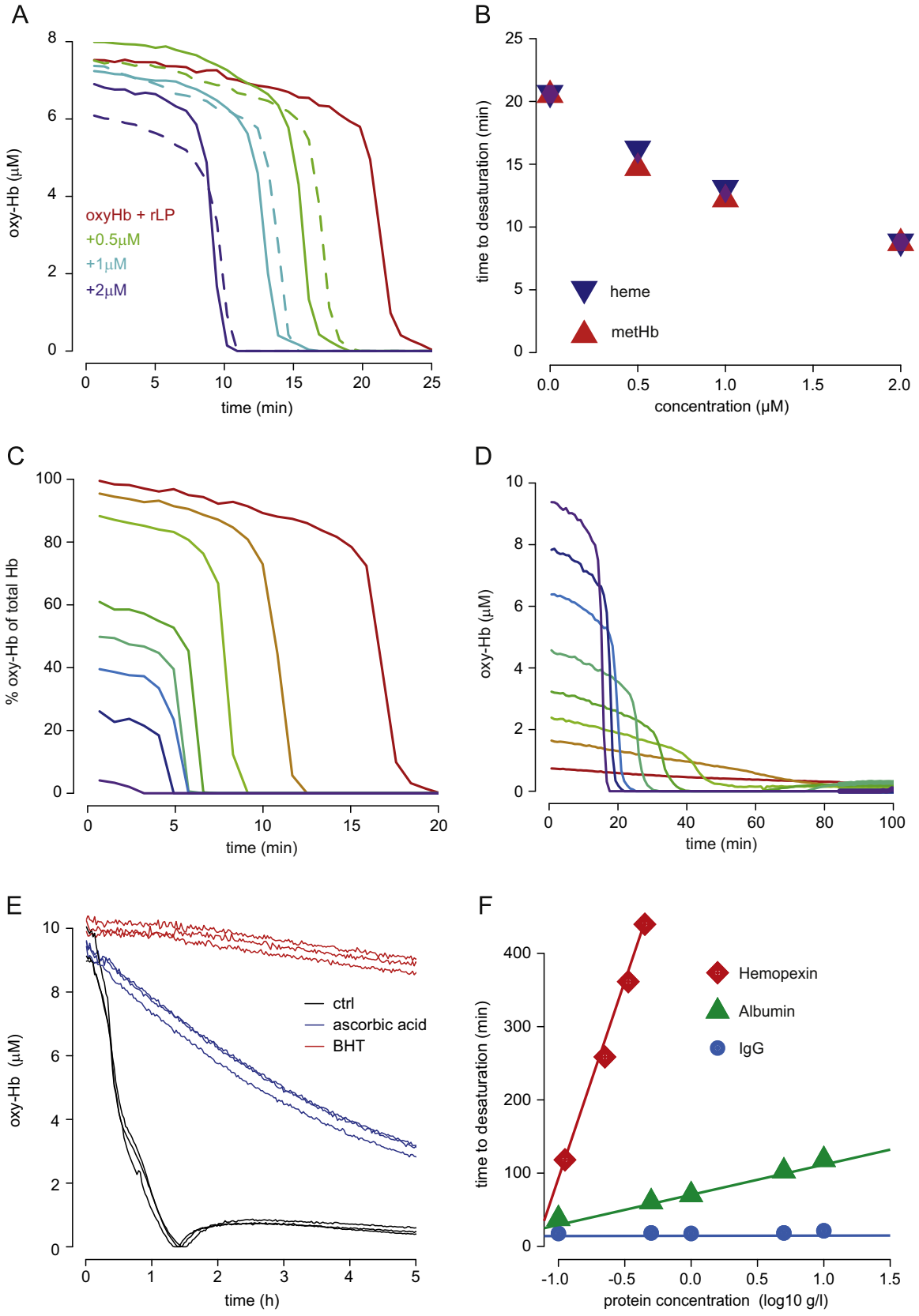

Fig. 5. Critical role of free heme in the oxyHb+rLP reaction. Deoxygenation of Hb was measured in the oxyHb catalyzed rLP oxidation reactions by spectrophotometry combined with multicomponent spectral deconvolution (rLP 0.5 g/L, in PBS pH 7.4, 37°C). A. Acceleration of oxyHb depletion (oxygen consumption in the reaction) by addition of either free heme (dashed lines) or ferric Hb (solid lines) to the rLP+Hb reaction (oxyHb 10 μM). B. Graphical representation of time to oxygen depletion versus concentration of added heme or ferric Hb of the experiment shown in Fig. 5A. C. 10 μM Hb was reacted with rLP. The different traces represent different fractional concentrations of oxyHb (plotted) and ferric Hb at the start of the reaction (time=0 min.) with the red trace representing a reaction with 100% oxyHb. Higher fractions of ferric Hb accelerated Hb deoxygenation. This is indicated by the sudden drop in oxyHb, which occurs earlier in reactions with a high ferric Hb fraction at the start of the reaction. D. rLP was incubated with different starting concentrations of oxyHb. In contrast to the experiment shown in Fig. 5C the oxyHb fraction was 100% in each reaction with no other heme/Hb species present. The red trace indicates the reaction with the lowest, the violet trace the reaction with the highest heme concentration. Higher concentrations of Hb accelerate the reaction velocity as indicated by an earlier oxyHb desaturation, which is indicated as a sudden drop of oxyHb. E. Effect of lipophilic and hydrophilic radical scavengers on oxyHb [Fe^{2+}] concentration during the oxyHb+rLP reaction. In this experiment, 10 μM oxyHb was reacted with 0.5 g/l rLP plus 20 μM sodium ascorbate, a hydrophilic antioxidant (blue), or 20 μM butylated toluene BHT (red), a lipophilic antioxidant. A sample lacking antioxidant was used as a control (black). F. 10 μM oxyHb were reacted with 0.5 g/l rLP in the presence of Hp, Hx, albumin, or bovine immunoglobulin at various protein concentrations.

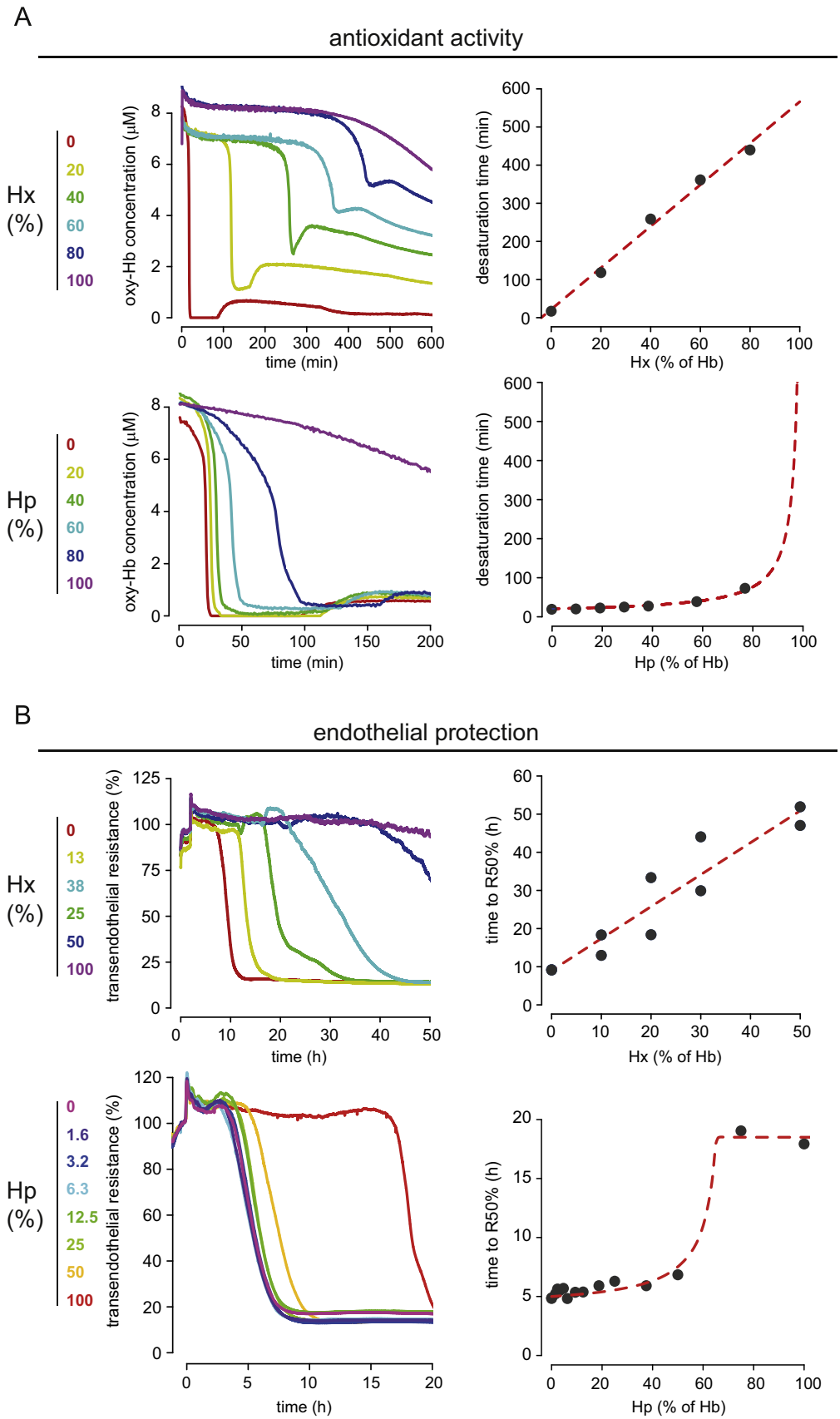

Fig. 6. Quantitative requirements for protection by Hp and Hx. A. 10 μM oxyHb were reacted with 0.5 g/l rLP in the presence of Hx (upper panel) or Hp (lower panel) over a range of scavenger protein concentrations between 0% and 100% scavenger capacity relative to heme (at 100% all heme is bound as a heme-Hx or Hb:Hp complex). oxyHb concentrations were determined over time by spectrophotometry and multicomponent spectral deconvolution. In the right panels the time to Hb desaturation of each sample is plotted against the scavenger protein capacity of Hx and Hp, respectively. B. Identical reactions as in (A) were performed in HUVEC cell culture and transendothelial electrical resistance was measured by ECIS (left panels). In the right panels the time to loss of 50% of the resistance was plotted against the scavenger protein capacity of Hx and Hp, respectively.

may therefore be considered as a free heme donor in this system (Fig. 5**B**). In another set of reactions, we replaced oxyHb (Fe^{2+}) stepwise with ferric Hb (Fe^{3+}), while keeping the total heme content constant throughout the reaction. Oxygen consumption, and thus rLP oxidation, was accelerated relative to the proportion of replaced oxyHb (Fig. 5**C**). In contrast, if the oxyHb (Fe^{2+}) concentration was reduced without replacement by ferric Hb (Fe^{3+}), the oxygen consumption and rLP oxidation rates became slower (Fig. 5**D**). These data further confirm that free heme is the catalyst of lipid peroxidation while ferric Hb (Fe^{3+}) acts as a donor of free heme. The reaction rate for Hb triggered ox-rLP formation is not determined by the concentration of oxyHb (Fe^{2+}), which is the primary species released from red blood cells, but by the concentration of releasable heme in ferric Hb (Fe^{3+}).

Further studies with lipophilic and hydrophilic radical scavengers suggested that the ultimate heme-lipid peroxidation reaction occurs in the lipid compartment of our system. Ascorbic acid, which only acts in the aqueous phase due to its hydrophilic functional groups, slowed the reaction, but did not inhibit it completely. In contrast, butylated hydroxytoluene (BHT), a non-polar lipophilic radical scavenger that accumulates exclusively in the rLP spheres, completely stopped the Hb-rLP reaction (Fig. 5**E**).

The protection provided by Hx is a specific biochemical function of this protein since the low-affinity heme scavenger albumin and non-heme-binding immunoglobulin demonstrate minimal to no effect on the oxidative reaction (Fig. 5**F**).

3.4. Quantitative analysis links target specificities of Hp and Hx to different stoichiometric requirements for protection

In a next set of experiments we quantitatively assessed the protective effects provided by the two scavenger proteins Hp and Hx when they were present in the lipid oxidation system at sub-stoichiometric concentrations relative to Hb. Hp slowed the rate of oxygen consumption and prevented endothelial monolayer disintegration. However, near stoichiometric concentrations of Hp relative to heme were required for attenuation of these biochemical and cellular changes (Fig. 6**A, B**). The mechanism of this protection is likely related to the structural stabilization of Hb within the complex, which prevents release of catalytically active heme in case the Hb:Hp complex may be transformed to ferric Hb (Fe^{3+}). The observation that near iso-stoichiometric Hp is required for protection can be explained by the lack of specificity of this scavenger for free heme (or ferric Hb) binding. Instead, the effect of Hp reduces the quantity of cumulative oxyHb (Fe^{2+}) and ferric Hb (Fe^{3+}) in the system and prevents heme loss from the bound ferric Hb fraction or when oxyHb:Hp complexes are converted to ferric. To further demonstrate this assumption we stepwise replaced of oxyHb (Fe^{2+}) in the reaction with Hb:Hp complexes while keeping the total heme concentration in the reaction constant (Supplemental Figure 1). These data confirm that the protection provided by addition of Hp equals the effect that can be observed by decreasing the oxyHb (Fe^{2+}) equivalents.

In contrast to Hp, Hx prolonged the time to oxygen depletion even at low (sub-stoichiometric) concentrations. In this case the time to Hb desaturation was linearly proportional to the Hx concentration (Fig. 6**A**). Moreover, Hx demonstrated a dose dependent protection of endothelial monolayer integrity (Fig. 6**B**). These experiments confirm that in states of oxyHb excess where a slow conversion to ferric Hb (Fe^{3+}) occurs, small amounts of Hx can effectively remove heme from the system. The major determinant of the protective capacity in this case is not the release of Hb from red blood cells but the oxidation of oxyHb (Fe^{2+}) to ferric Hb (Fe^{3+}).

Cumulatively, our data suggest that the different target specificities of Hp and Hx determine their stoichiometric requirements when added to a complex system with Hb-triggered lipid peroxidation reactions and downstream cytotoxicity. As a final experimental illustration of this concept, we measured the accumulation of thiobarbituric acid reactive substances (TBARS) following reaction with fixed concentrations of rLP (0.5 g/L), Hp (10 μM), Hx (5 μM), and Hp+Hx (10 μM+5 μM) along a oxyHb concentration range of 0–100 μM. This experimental design enabled evaluation of the pro-oxidant effects of sub-stoichiometric to supra-stoichiometric Hb concentrations relative to the scavenger proteins (Fig. 7**A**). In the absence of either Hp or Hx, TBARS formation was dependent solely on the amount of Hb present in the reaction. Addition of Hp completely blocked lipid peroxidation until the Hb concentration exceeded a 1:1 (Hb:Hp) stoichiometry. Above this concentration threshold, when Hp was saturated, TBARS formation followed an Hb dose-response curve that was identical to the control reaction, which lacked Hp. In contrast, Hx inhibited TBARS formation up to a 11-fold molar excess of oxyHb (Fe^{2+}), demonstrating its ability to effectively remove heme from the reaction at sub-stoichiometric concentrations relative to Hb. If both Hp and Hx were added to the reaction simultaneously, the effect of Hx on TBARS formation was extended exactly by the concentration of Hp, indicating that Hx activity was spared until the point at which Hp became saturated.

In an identical experiment as shown above we investigated whether the specific lipid peroxidation product 4-hydroxynnonenal (4-HNE) is generated during the Hb reaction with rLP. Fig. 7**B** shows a Western blot for 4-HNE alongside a total protein stain. The experiment shows that a range of heterogeneous 4-HNE protein-adducts are produced in the reaction of oxyHb(Fe^{2+}) (50 μM) with rLP (0.5 g/L), while the protein components of Hb and rLP (ApoA1) disappear, presumably as a result of protein crosslinking and lipid peroxide adduction. In agreement with the TBARS experiments, substoichiometric heme binding quantities of Hx (10 μM) prevent these reactions, while higher heme-binding equivalent concentrations of Hp (50 μM) are required to have the same protective effect.

4. Discussion

In this paper, we provide a biochemical model that rationalizes the role of Hp as a primary protection system, which controls all adverse activities of free Hb. Once Hp is depleted, Hx functions as a backup protection system providing sustained control of Hb-driven oxidative damage (Fig. 7**B**). These results are consistent with and provide a mechanistic rationale for the observations of a sequential depletion pattern observed for these two scavenger proteins in patients with hemolytic conditions [12,31].

To support the hypothesis that different stoichiometric requirements for oxidative protection by Hp and Hx mediate their global role as primary and backup control systems, we developed an in vitro model that allowed us to quantify, compare, and correlate the biochemical activity and endothelial protective capacity of the two scavenger proteins. In contrast to earlier models, including our own model of Hb oxidation and endothelial damage [21], this new model is driven by a reaction of oxyHb (Fe^{2+}) with a biochemically defined lipoprotein in the absence of additional oxidants such as H_2O_2. This model may be more reflective of most conditions associated with hemolysis, in which only a small fraction of the total oxyHb that is released from erythrocytes is slowly transformed from the oxyHb (Fe^{2+}) state into ferric Hb (Fe^{3+}) by autoxidation or reaction with oxidants such as NO [9]. Only this small fraction of Hb (Fe^{3+}) can release its heme and eventually trigger lipid oxidation and endothelial damage. This pathophysiologic sequence with heme as the ultimate trigger of lipid oxidation provides the basis for our

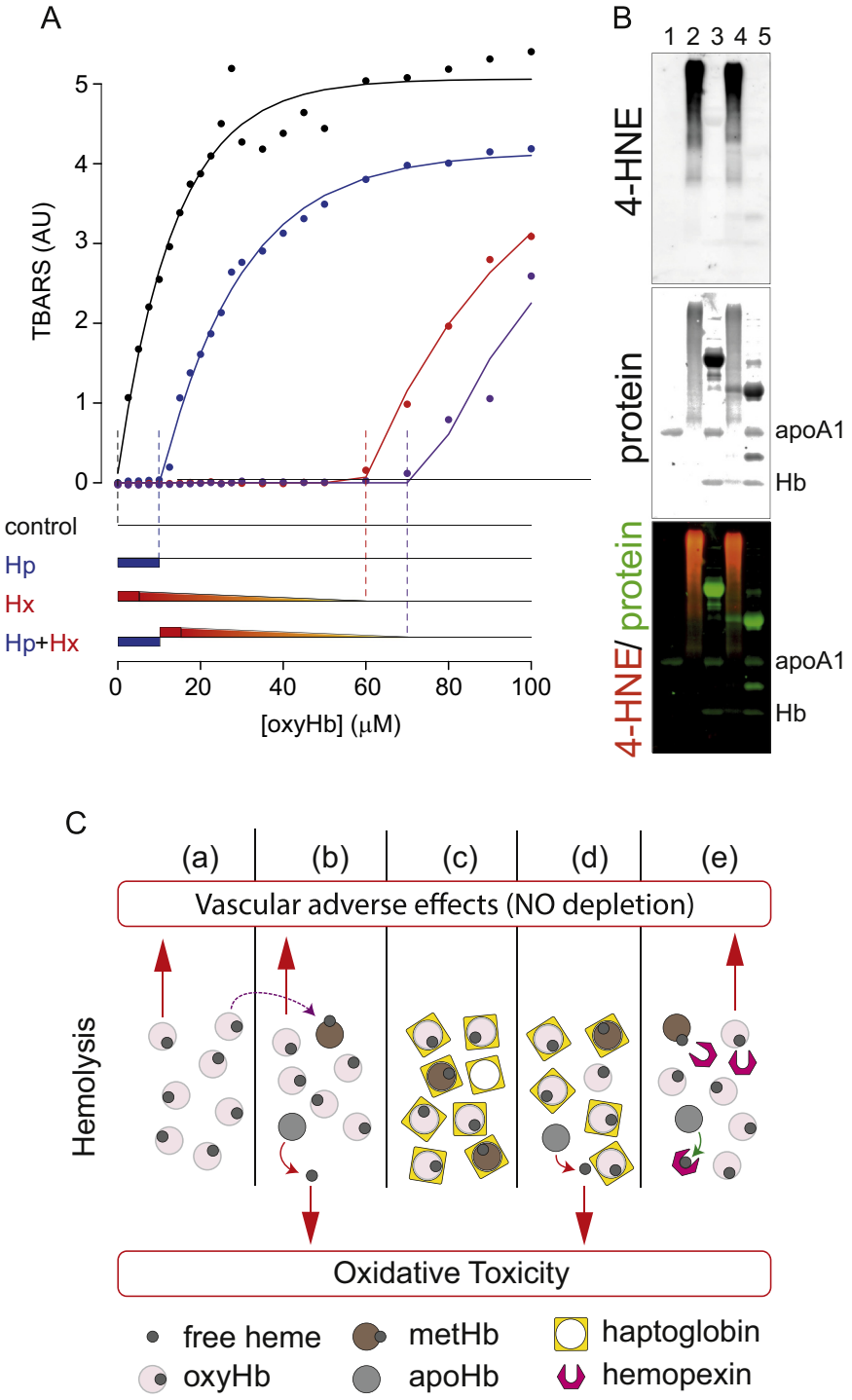

Fig. 7. Quantitative requirements differ between Hp and Hx for the prevention of lipid peroxidation. A. In this experiment 0.5 g/l rLP was incubated with a range of oxyHb concentrations for 120 min at 37°C in PBS pH 7.4 in the absence or presence of Hp (10 μM heme-binding equivalent), Hx (5 μM heme-binding equivalent) or both scavengers. TBARS where measured at 590 nm fluorescence (excited at 540 nm). B. Western blot for 4-HNE (red fluorescence channel). Total protein is shown in the green fluorescence channel. 1: (only 0.5 g/L rLP), 2: (rLP+50 μM Hb), 3: (rLP+50 μM Hb+10 μM hemopexin), 4: (rLP+50 μM Hb+10 μM haptoglobin), 5: (rLP+50 μM Hb+50 μM haptoglobin). C. Schematic of the different protective mechanisms provided by Hp and Hx relative to their stoichiometry. (a) oxyHb depletes NO, which causes vasoconstriction and a hypertensive response. Autooxidation and reaction with NO and other oxidants convert oxyHb to metHb (step 1). (b) metHb triggers oxidative toxicity by heme release (step 2). (c) As long as enough haptoglobin is available to associate with extracellular Hb, both toxicity mechanisms are blocked and Hb toxicity is prevented. Once Hb exceeds the Hp concentration, heme can be released from even small quantities of unbound ferric Hb (step 3) to induce oxidative toxicity. (e) In contrast to Hp, Hx forms complexes with free heme (step 4) without any significant consumption by the excess oxyHb. Hx is therefore able to delay oxidative Hb toxicity even during conditions with massive Hb release that exceeds the concentrations of scavenger proteins.

observation that the heme specific scavenger Hx is functional to prevent heme toxicity in experimental conditions with vast excess of oxyHb (Fe^{2+}). Hp can also limit free heme availability by its function as a structural stabilizer of the Hb molecule, which blocks heme-release. However, Hp lacks specificity for the oxidative active component (i.e. ferric Hb or free heme), which is reflected by the high concentrations of Hp relative to Hb that were required in our model to effectively block the toxic cascade.

Our data demonstrate that protective functions were linked to Hx concentration with a linear function. This linear relationship explains the observation that Hx significantly delays the toxic effects of heme even at sub-stoichiometric concentrations relative to oxyHb. Conversely, the biochemical role of Hp within this context correlated to Hb concentration in an exponential manner, supporting the requirement of 1:1 stoichiometric concentrations of Hp relative to Hb (Fe^{2+}) for effective modulation of lipid peroxidation and attenuation of endothelial damage.

The differential quantitative requirements of Hp and Hx for effective control of lipid peroxidation were also confirmed in a second model in which the accumulation of lipid peroxidation products (TBARS and 4-HNE adducts) was directly quantified as a function of the Hb to scavenger protein ratio **(**Fig. 7**A)** instead of the time period to the appearance of predefined markers of lipid oxidation and endothelial damage. In these experiments we demonstrate that Hx prevented TBARS formation when Hb concentrations exceed the concentration of the scavenger by more than ten-fold. In contrast, because Hp's mode of action simply "reduces" the amount of Hb that could potentially release its heme moiety after Hb (Fe^{3+}) transformation by exactly the fraction bound in the Hb:Hp complex, Hp could not block lipid peroxidation beyond Hb concentrations exceeding the binding capacity of Hp.

When both Hp and Hx were present in the system, we observed a right-shift of the TBARS formation curve that corresponded exactly to the heme equivalent binding capacity of added Hp. This observation supports another important aspect of the sequential protection-depletion model. During free Hb exposure, the Hb-heme stabilizing function of Hp provides not only a first-line of protection against Hb-triggered lipid peroxidation, but it also supports that Hx is spared until the capacity of the primary protection system is exhausted.

The sequential Hb scavenger protein protection-depletion model allows for an adapted control of Hb adverse effects in different disease conditions with varying activity and duration of hemolysis [1]. In conditions with mild hemolysis or during short episodes of acute hemolysis, Hp can control Hb vasoactivity – which is driven by oxyHb($Fe^{2+}O_2$) mediated NO depletion – in addition to the prevention of renal Hb filtration, and oxidative tissue damage. However, this control of Hb toxicity comes at the cost of very high scavenger consumption that can cause Hp depletion within hours. The backup scavenger, Hx, cannot control vasoactivity and extravasation of Hb. However, a limited quantity of Hx provides prolonged control of heme-triggered oxidative tissue damage **(**Fig. 7**B)** [11]. The endocytic recycling of apo-Hx by liver cells may further support the prolonged protection provided by Hx when Hp is depleted [32]. In contrast, Hp is degraded by macrophages after endocytosis of the Hb:Hp complex by the macrophage scavenger receptor CD163 [33]. The heme defense role of Hx is also supported by other lower affinity heme-binding plasma proteins, which may either serve as a temporary reservoir for free heme before it is neutralized by Hx, or which may provide a third line of defense when all Hx is consumed. Such alternative heme-binding proteins are albumin (K_d) 10^{-8} M [34] and a1-microglobulin (K_d.10^{-6}M) [35]. In contrast, the hexacoordinate high affinity heme-binding by Hx has a $K_d < 10^{-13}$M [36].

Hp and Hx are being considered as therapeutics for various hemolytic conditions. While the biochemical functions of the two proteins are broadly overlapping in certain disease models [3], the principles of our model, designed to understand the combined functional contribution of each scavenger in Hb/heme detoxification, may help guide selection of the most appropriate scavenger for future experimental and/or hemolytic disease state specific clinical studies. For example, administration of Hp at large doses that match the quantity of Hb release may be the preferred therapy for treating acute, intense episodes of intravascular hemolysis. During acute hyperhemolysis, Hp may provide the most effective approach to limiting kidney and cardiovascular system injury. However, the requirements of Hp are considerable. For examples, the total endogenous pool of plasma Hp of an adult person is about 3 g. This amount of Hp may only neutralize about 0.5% of the total RBC Hb, which indicates that even supplementation of 10-fold the endogenous Hp may neutralize no more than an amount of Hb corresponding to acute hemolysis of 5% of total RBC. In patients it may, therefore, not be possible to supplement protective Hp plasma concentrations for prolonged periods in chronic hemolytic states, such as in patients with sickle cell disease. Under these conditions, regular administration of limited doses of Hx may allow sustained and selective protection against pro-oxidant-mediated tissue injury. Estimating effective therapeutic doses is much more difficult for Hx than for Hp, because Hx requirements will not be directly related to the rate of hemolysis but much more to the rate of in vivo transformation of ferrous to ferric Hb as well to the kinetics of Hx recycling. However, the general concept that different quantities of the two scavenger proteins may provide differential protection in hemolytic conditions has already found experimental support in recent animal studies. For example, repeated administration of low doses of Hx (1 mg per animal/week) to sickle cell mice was effective in attenuating vascular oxidative damage [11]. In contrast, large single bolus doses of Hp were required in other studies to attenuate the acute renal and vascular toxicity that emerged after transfusion of stored blood with acute intravascular release of free Hb in large quantities [9].

In conclusion, we provide an experimental model that links the roles of Hp and Hx as primary and backup protection systems with the specific quantum requirement of each scavenger protein to effectively control free Hb-triggered oxidative damage.

AUTHORSHIP CONTRIBUTIONS

JWD and DJS designed the study, performed experiments, analyzed data, and wrote the manuscript. FV designed the study and performed experiments. CAS and MP performed experiments, and PWB designed the study and wrote the manuscript. The authors declare no conflict of interest.

ACKNOWLEDGMENTS

This work was supported by the Swiss National Science Foundation (grants 310030/120658 and 31003A/138500 to DJS), the University of Zurich Research Priority Program "Integrative Human Physiology" and the Swiss Federal Commission for Technology and Innovation (CTI).

Appendix A. Supplementary material

Supplementary data associated with this article can be found in the online version at http://dx.doi.org/10.1016/j.freeradbiomed.2015.09.016.

References

[1] D.J. Schaer, P.W. Buehler, A.I. Alayash, J.D. Belcher, G.M. Vercellotti, Hemolysis and free hemoglobin revisited: exploring hemoglobin and hemin scavengers as a novel class of therapeutic proteins, Blood 121 (2013) 1276–1284.
[2] M.T. Gladwin, T. Kanias, D.B. Kim-Shapiro, Hemolysis and cell-free hemoglobin

drive an intrinsic mechanism for human disease, J Clin Invest 122 (2012) 1205–1208.
[3] J.D. Belcher, C. Chen, J. Nguyen, L. Milbauer, F. Abdulla, A.I. Alayash, A. Smith, K. A. Nath, R.P. Hebbel, G.M. Vercellotti, Heme triggers TLR4 signaling leading to endothelial cell activation and vaso-occlusion in murine sickle cell disease, Blood 123 (2014) 377–390.
[4] F.F. Dutra, L.S. Alves, D. Rodrigues, P.L. Fernandez, R.B. de Oliveira, D. T. Golenbock, D.S. Zamboni, M.T. Bozza, Hemolysis-induced lethality involves inflammasome activation by heme, Proceedings of the National Academy of Sciences of the United States of America 111 (2014) E4110–E4118.
[5] F.F. Dutra, M.T. Bozza, Heme on innate immunity and inflammation, Frontiers in pharmacology 5 (2014) 115.
[6] V. Jeney, G. Balla, J. Balla, Red blood cell, hemoglobin and heme in the progression of atherosclerosis, Frontiers in physiology 5 (2014) 379.
[7] M. Lipiski, J.W. Deuel, J.H. Baek, W.R. Engelsberger, P.W. Buehler, D.J. Schaer, Human Hp1-1 and Hp2-2 phenotype-specific haptoglobin therapeutics are both effective in vitro and in guinea pigs to attenuate hemoglobin toxicity, Antioxidants & redox signaling 19 (2013) 1619–1633.
[8] E. Tolosano, S. Fagoonee, N. Morello, F. Vinchi, V. Fiorito, Heme scavenging and the other facets of hemopexin, Antioxidants & redox signaling 12 (2010) 305–320.
[9] J.H. Baek, F. D'Agnillo, F. Vallelian, C.P. Pereira, M.C. Williams, Y. Jia, D.J. Schaer, P.W. Buehler, Hemoglobin-driven pathophysiology is an in vivo consequence of the red blood cell storage lesion that can be attenuated in guinea pigs by haptoglobin therapy, J Clin Invest 122 (2012) 1444–1458.
[10] F.S. Boretti, P.W. Buehler, F. D'Agnillo, K. Kluge, T. Glaus, O.I. Butt, Y. Jia, J. Goede, C.P. Pereira, M. Maggiorini, G. Schoedon, A.I. Alayash, D.J. Schaer, Sequestration of extracellular hemoglobin within a haptoglobin complex decreases its hypertensive and oxidative effects in dogs and guinea pigs, J Clin Invest 119 (2009) 2271–2280.
[11] F. Vinchi, L. De Franceschi, A. Ghigo, T. Townes, J. Cimino, L. Silengo, E. Hirsch, F. Altruda, E. Tolosano, Hemopexin therapy improves cardiovascular function by preventing heme-induced endothelial toxicity in mouse models of hemolytic diseases, Circulation 127 (2013) 1317–1329.
[12] U. Muller-Eberhard, J. Javid, H.H. Liem, A. Hanstein, M. Hanna, Plasma concentrations of hemopexin, haptoglobin and heme in patients with various hemolytic diseases, Blood 32 (1968) 811–815.
[13] D.J. Schaer, F. Vinchi, G. Ingoglia, E. Tolosano, P.W. Buehler, Haptoglobin, hemopexin, and related defense pathways-basic science, clinical perspectives, and drug development, Frontiers in physiology 5 (2014) 415.
[14] D.J. Schaer, P.W. Buehler, Cell-free hemoglobin and its scavenger proteins: new disease models leading the way to targeted therapies, Cold Spring Harbor perspectives in medicine 3 (2013).
[15] G. Balla, G.M. Vercellotti, U. Muller-Eberhard, J. Eaton, H.S. Jacob, Exposure of endothelial cells to free heme potentiates damage mediated by granulocytes and toxic oxygen species, Laboratory investigation; a journal of technical methods and pathology 64 (1991) 648–655.
[16] G. Balla, H.S. Jacob, J.W. Eaton, J.D. Belcher, G.M. Vercellotti, Hemin: a possible physiological mediator of low density lipoprotein oxidation and endothelial injury, *Arteriosclerosis and thrombosis*: a journal of vascular *biology / American Heart Association* 11 (1991) 1700–1711.
[17] J. Balla, H.S. Jacob, G. Balla, K. Nath, J.W. Eaton, G.M. Vercellotti, Endothelial-cell heme uptake from heme proteins: induction of sensitization and desensitization to oxidant damage, Proceedings of the National Academy of Sciences of the United States of America 90 (1993) 9285–9289.
[18] V. Jeney, J. Balla, A. Yachie, Z. Varga, G.M. Vercellotti, J.W. Eaton, G. Balla, Pro-oxidant and cytotoxic effects of circulating heme, Blood 100 (2002) 879–887.
[19] E. Nagy, V. Jeney, A. Yachie, R.P. Szabo, O. Wagner, G.M. Vercellotti, J.W. Eaton, G. Balla, J. Balla, Oxidation of hemoglobin by lipid hydroperoxide associated with low-density lipoprotein (LDL) and increased cytotoxic effect by LDL oxidation in heme oxygenase-1 (HO-1) deficiency, Cellular and molecular biology 51 (2005) 377–385.
[20] E. Nagy, J.W. Eaton, V. Jeney, M.P. Soares, Z. Varga, Z. Galajda, J. Szentmiklosi, G. Mehes, T. Csonka, A. Smith, G.M. Vercellotti, G. Balla, J. Balla, Red cells, hemoglobin, heme, iron, and atherogenesis, Arteriosclerosis, thrombosis, and vascular biology 30 (2010) 1347–1353.
[21] C.A. Schaer, J.W. Deuel, A.G. Bittermann, I.G. Rubio, G. Schoedon, D.R. Spahn, R. A. Wepf, F. Vallelian, D.J. Schaer, Mechanisms of haptoglobin protection against hemoglobin peroxidation triggered endothelial damage, Cell death and differentiation 20 (2013) 1569–1579.
[22] F. D'Agnillo, A.I. Alayash, Site-specific modifications and toxicity of blood substitutes. The case of diaspirin cross-linked hemoglobin, Advanced drug delivery reviews 40 (2000) 199–212.
[23] G. Silva, V. Jeney, A. Chora, R. Larsen, J. Balla, M.P. Soares, Oxidized hemoglobin is an endogenous proinflammatory agonist that targets vascular endothelial cells, The Journal of biological chemistry 284 (2009) 29582–29595.
[24] T. Pimenova, C.P. Pereira, P. Gehrig, P.W. Buehler, D.J. Schaer, R. Zenobi, Quantitative mass spectrometry defines an oxidative hotspot in hemoglobin that is specifically protected by haptoglobin, Journal of proteome research 9 (2010) 4061–4070.
[25] F. Vallelian, I. Garcia-Rubio, M. Puglia, A. Kahraman, J.W. Deuel, W. R. Engelsberger, R.P. Mason, P.W. Buehler, D.J. Schaer, Spin trapping combined with quantitative mass spectrometry defines free radical redistribution within the oxidized hemoglobin:haptoglobin complex, Free radical biology & medicine 85 (2015) 259–268.
[26] Y.I. Miller, A. Smith, W.T. Morgan, N. Shaklai, Role of hemopexin in protection of low-density lipoprotein against hemoglobin-induced oxidation, Biochemistry 35 (1996) 13112–13117.
[27] P.G. Lerch, V. Fortsch, G. Hodler, R. Bolli, Production and characterization of a reconstituted high density lipoprotein for therapeutic applications, Vox sanguinis 71 (1996) 155–164.
[28] C.A. Schaer, G. Schoedon, A. Imhof, M.O. Kurrer, D.J. Schaer, Constitutive endocytosis of CD163 mediates hemoglobin-heme uptake and determines the noninflammatory and protective transcriptional response of macrophages to hemoglobin, Circulation research 99 (2006) 943–950.
[29] G.R. Kelman, Digital computer subroutine for the conversion of oxygen tension into saturation, Journal of applied physiology 21 (1966) 1375–1376.
[30] V. Matyash, G. Liebisch, T.V. Kurzchalia, A. Shevchenko, D. Schwudke, Lipid extraction by methyl-tert-butyl ether for high-throughput lipidomics, Journal of lipid research 49 (2008) 1137–1146.
[31] U. Muller-Eberhard, Hemopexin, The New England journal of medicine 283 (1970) 1090–1094.
[32] A. Smith, W.T. Morgan, Haem transport to the liver by haemopexin. Receptor-mediated uptake with recycling of the protein, The Biochemical journal 182 (1979) 47–54.
[33] M.J. Nielsen, H.J. Moller, S.K. Moestrup, Hemoglobin and heme scavenger receptors, Antioxidants & redox signaling 12 (2010) 261–273.
[34] P.A. Adams, M.C. Berman, Kinetics and mechanism of the interaction between human serum albumin and monomeric haemin, The Biochemical journal 191 (1980) 95–102.
[35] J. Larsson, M. Allhorn, B. Kerstrom, The lipocalin alpha(1)-microglobulin binds heme in different species, Archives of biochemistry and biophysics 432 (2004) 196–204.
[36] W.T. Morgan, H.H. Liem, R.P. Sutor, U. Muller-Ebergard, Transfer of heme from heme-albumin to hemopexin, Biochimica et biophysica acta 444 (1976) 435–445.